Materials and Design 66 (2015) 366–375

Contents lists available at ScienceDirect

Materials and Design

journal homepage: www.elsevier.com/locate/matdes

Grain refinement of Al–Si alloys by Nb–B inoculation. Part I: Concept development and effect on binary alloys

M. Nowak, L. Bolzoni *, N. Hari Babu

BCAST (Brunel Centre for Advanced Solidification Technology), Brunel University, Uxbridge, Middlesex UB8 3PH, UK

ARTICLE INFO

Article history:
Received 15 July 2014
Accepted 21 August 2014
Available online 6 September 2014

Keywords:
Al alloys
Binary alloys
Grain refinement
Heterogeneous nucleation
Nb–B inoculation

ABSTRACT

The effect of Nb–B inoculation on Al–Si alloys for their grain refinement has been studied through the analysis of binary Al–*x*Si (where *x* = 1–10 wt.%) to avoid possible effects of other alloying elements. In Part I of this work the concept development of the Nb–B inoculation is discussed in detail on the basis of the theoretical and fundamental concepts employed (i.e. pro-peritectic particles formation, lattice structures and mismatch as well as analogies between the Al–Ti/Al–Nb or Ti–Si/Nb–Si binary phase diagrams). The systematic study of the addition of different level of Nb–B inoculation to pure Al permitted to determine the best addition rate. From the microstructural and thermal analysis of binary Al–*x*Si alloys it is found that Nb–B inoculation is highly suitable for Al–Si alloy with Si content greater than 6 wt.%. As results of the Nb–B inoculation the microstructural features of binary Al–*x*Si alloys (i.e. primary Al α-grains and eutectic phase) are significantly refined. Most importantly, the inoculation of Al–Si cast alloys with Nb–B is not characterised by any visible poisoning effect (i.e. formation of silicides) which is the drawback of using commercial Al–Ti–B master alloys on Al cast alloys. The effect of Nb–B inoculation on commercial Al–Si alloys (which normally include other alloying elements in their chemical composition) is assessed in Part II of this work.

1. Introduction

Aluminium and its alloys are common engineering materials for structural applications due to the combination of properties they can provide. Specifically: low density (2.7 g/cm^3), corrosion resistance in many environments, good specific strength (i.e. strength to density ratio), good thermal conductivity and low electrical resistivity. As for other metals, the primary process employed to fabricate Al alloys is used to differentiate and categorise them as wrought and cast. Cast Al alloys are based on the binary Al–Si phase diagram and are used because of their low melting point, good fluidity, good surface finishing as well as limited solubility for gases (except for hydrogen). Other alloying elements such as magnesium and copper are generally contemplated in the alloy composition to achieve specific properties like improved corrosion resistance or better response to heat-treatments. Depending on the production route employed, Al can be characterised by quite coarse microstructure and, thus, its grain refinement it is a common industrial practise [1]. Usually, the grain refinement is carried out by the addition of commercial master alloy developed and based on the ternary Al–Ti–B system, such as the Al–5Ti–1B master alloy, which is added to the melt prior casting [2–5]. It is worth mentioning that Ti is the elements with the highest growth restriction factor [6], which plays an important role in the refinement of Al by means heterogeneous nucleation. The mechanism behind the grain refinement of Al has been a topic of debate and various theories were proposed: phase diagram/peritectic theory, peritectic hulk theory, hypernucleation theory, and solute theory [7–9]. Summarising, the employment of commercial Al–Ti–B master alloy is based on the scientific fundamental that Ti reacts with B forming TiB_2 particles and with Al forming Al_3Ti intermetallic particles. When the commercial master alloy is added to the molten Al, TiB_2 particles act as heterogeneous nucleation sites whilst Al_3Ti intermetallics dissolve into the melt on the base of the peritectic reaction forming α-Al: liquid $Al + Al_3Ti \rightarrow$ α-Al (solid solution) [9,10]. Observation of the interface Al_3Ti layer on TiB_2 particles suggested that TiB_2 particles in combination with Al_3Ti contribute to the heterogeneous nucleation of α-Al grains [11]. Commercial Al–Ti–B master alloy are very potent grain refiners for wrought Al alloys, whose Si content is generally lower than 2 wt.%. Nonetheless, in the case of cast Al alloys, where Si content is greater than 4 wt.%, the efficiency of commercial Al–Ti–B master alloys is relatively poor. This is due to the interaction of Ti with Si to form titanium silicides (i.e. TiSi, $TiSi_2$ and Ti_5Si_3) which depletes the melt

* Corresponding author.
E-mail address: leandro.bolzoni@brunel.ac.uk (L. Bolzoni).

http://dx.doi.org/10.1016/j.matdes.2014.08.066
0261-3069/

of Ti preventing the grain refinement of the alloy. This phenomenon has been the subject of different studies and it is known as poisoning effect [4,12–14]. Many attempts and a lot of effort have been focused in achieving fine equiaxed grain structure in as-cast Al–Si alloys by the addition of small quantities of elements called hardeners (which includes Zr, Nb, V, W, Ta, Ce, etc. [15–19]) but without much success. The latest works focused on the effect of commercial Al–B master alloys (i.e. Al–3B), Al–Ti–C master alloys [20], Al–Ti–B–C master alloys [21] or variants of the Al–Ti–B master alloys [22,23]. The most significant result of research done by Birol [24] is that the Al–3B master alloy performs very well in refining Al–Si alloys grain structure when they are Ti-free, which is not the case for most of the Al cast alloys. When Ti is present as impurity in percentage greater than 0.04 wt.% the Al–3B master alloy refining potency is equal to that of commercial master alloys based on the Al–Ti–B ternary system (i.e. Al–5Ti–1B and Al–3Ti–3B) [24]. Potential heterogeneous nucleation substrates for grain refinement have to be characterised by three main aspects [25]: (1) high melting temperature to prevent their melting when placed in contact with the molten metal to be refined, (2) low lattice mismatch with the nucleating phase and (3) chemically stability (do not interact with the alloying elements). The aim of this work is to report and discuss the grain refinement of Al–Si cast alloys by Nb–B inoculation, chemical composition which was patented [26,27]. In particular, the concept development and the effect of Nb–B inoculation in binary Al–*x*Si alloys (where $x = 1–10$ wt.%) are discussed in Part I. Binary Al–Si alloys were chosen because they permitted to quantify the effect of Nb–B inoculation on the microstructural features (primary α-Al dendrites and secondary eutectic phase) without the concern of possible side effects of other alloying elements present in commercial Al–Si cast alloys. The effect of the addition of the Nb–B grain refiner to commercial Al–Si cast alloys solidified over a great range of cooling rates as well as the mechanism governing their grain refinement are assessed in Part II of this work.

2. Experimental procedure

The work described in this paper is divided into three main sections, namely (1) the study of the addition of Nb to commercial pure Al, (2) the study of the addition of interstitials (B and C) to the Al–Nb system and (3) the study of the addition of the 0.1Nb–0.1B to Al–*x*Si binary alloys. Therefore, at each specific time different materials and methods were used. Nevertheless, the general path followed is reported in this section and it is applicable for the experiments described unless otherwise specified. The raw materials employed were:

- Commercial pure Al (Al > 99.5 wt.%, Si = 0.02 wt.%, Fe = 0.08 wt.%, Mn = 0.01 wt.%, Zn = 0.02 wt.%, Ti = 0.06 wt.% and Ga = 0.05 wt.%) supplied by Norton Aluminium: used to test the refining potency of Nb and Nb–B as well as for the production of binary Al–*x*Si alloys, where $x = 1–10$ wt.%.
- Al–50Si master alloy: mixed with pure Al to produce binary Al–*x*Si alloys, where $x = 1–10$ wt.%. The Al–*x*Si alloys were produced in batches of 5 kg and their chemical composition was checked by means of an appositely calibrated FOUNDRY-MASTER Pro equipment (Oxford Instruments).
- Nb powders (Nb > 99.8%) with big particle size (average particle size 100 μm) and with fine particle size (lower than 45 μm) procured from Alfa Aesar. Initially (Section 3.1.2) the coarse Nb powder was used and it was found that it shows poor dissolution into Al although it permitted to study the sedimentation of Nb particles. Subsequently (from Section 3.1.3 onwards) all the experiments were carried out using the fine Nb powder. The total amount of Nb added varied during the development of the composition of the novel Nb–B grain refiner (Fig. 6) but it was then set to 0.1 wt.% (targeted addition) during the study of its performances on Al–*x*Si alloys.
- B powder (B > 98%) with particle size lower than 45 μm: initially used to study the combined effect of Nb and B on pure Al (Section 3.2.2). Lately (from Section 3.2.3 onwards), switched the potassium tetrafluoroborate (KBF_4) due to the non-wetting behaviour of the B powder which hinders its dissolution into the melt. Once again, the amount of B added to the melt was changed during the initial experiment (Fig. 6) but then fixed at 0.1. wt.% (targeted addition) during the study of the performances of Nb–B inoculation. It is worth mentioning that, although 0.1 wt.% was targeted, the actual content of Nb–B, measured by ICP method, is lower due to partial oxidation of the Nb powder during addition to the melt, low B recovery from KBF_4 and non-optimised mixing process.
- Potassium tetrafluoroborate (KBF_4 > 98%) flux purchased from Alfa Aesar: employed as alternative source of B.
- Graphite powder with particle size lower than 20 μm: employed to study the combined effect of Nb and C on pure Al.
- Commercial Al–5Ti–1B master alloy supplied by London & Scandinavian Metallurgical Co Limited: used to compare the performance and efficiency of Nb–B inoculation. The amount of master alloy added was equal to 0.1 wt.% which is a common percentage employed at industrial level.

Pure Al and binary Al–*x*Si alloys (where $x = 1–10$ wt.%) were melted and/or prepared in clay-bonded graphite crucibles and maintained at temperature for, at least, one hour. The melting temperature changed depending on the type of experiment (i.e. production of the binary Al–*x*Si alloy or grain refinement) and it varied between 720 °C and 800 °C. Specifically, 800 °C was mainly used when the addition of the Nb–B inoculant was considered. In the case of the pouring temperature, this parameter ranges between 660 °C and 720 °C depending on the nature of the experiments (i.e. study of the influence of the casting temperature). In some cases (e.g. study of the effect of the refiner on the base of the thermal analysis) the melt was left to cool inside a crucible externally lined with a glass wool insulator which permitted a very slow cooling rate (i.e. ~0.3 °C/s). The cast samples were prepared for metallographic analysis by using the classical route. In the case of macroanalysis, samples were grinded and etched by means of Tuckers' reagent whereas for microstructural analysis the samples were fine polished with OPS and characterised by means of an optical microscope (Carl Zeiss Axioscope A1) and/or SEM (Zeiss Supra 35VP FEG). The TP-1 test (Standard Test Procedure for Aluminum Alloy Grain Refiners) of The Aluminium Association [28] was used to compare the grain refinement efficiency because it permits to maintain a constant cooling rate and to determine the effect of the heterogeneous nucleation induced by the addition of grain refiners (cooling rate is ~3.5 °C/s). Grain size measurements were carried out on the base of the intercept method as per ASTM: E112. Cooling curves from liquid to solid of the selected composition were measured with K-type thermocouples and recorded by means of dedicated software (NI-VI Logger) collecting 100 data per second.

3. Results and discussion

3.1. Study of the addition of Nb to commercial pure Al

3.1.1. Analogies/differences between the Al–Ti and Al–Nb binary systems

Nb is a promising candidate for the refinement of Al and its alloys because, like Ti, it is characterised by a peritectic reaction

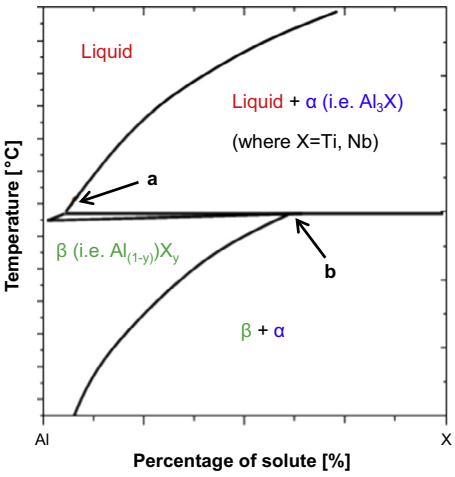

Fig. 1. Sketch of the Al-rich part of an Al–X binary phase diagram (percentage of solute at A: 0.15 wt.% of Ti or 0.15 wt.% of Nb and percentage of solute at B: 1.15 wt.% of Ti or 0.22 wt.% of Nb.

with Al. Moreover, Nb forms isostructural phases [29] to titanium aluminide, specifically Al_3Ti and Al_3Nb. Fig. 1 shows a sketch of the Al-rich part of Al–X (where X = Ti, Nb, etc.) binary phase diagram to emphasise the peritectic reaction. In the case of the Al–Ti phase diagram, Ti and Al react to form the Al_3Ti intermetallic at 665 °C. This compound has a tetragonal structure based on an ordered cubic close packed structure [30] (Ti content of 0.12–1.15 [29]). Nb has a very similar behaviour because the Al–Nb phase diagram is characterised by a peritectic reaction at approximately 661 °C and (Nb content of 0.15–0.22).

From Table 1, Nb is characterised by a body-centred cubic (B.C.C.) structure with lattice parameters similar to those of Al and/or Ti. These data are important to calculate the lattice mismatch, which was done by following Bramfil work [31]:

$$\delta_{(hkl)_n}^{(hkl)_s} = \sum_{i=1}^{3} \frac{\frac{|(d[uvw]_s^i \cos\theta) - d[uvw]_n^i|}{d[uvw]_n^i}}{3} \times 100 \quad (1)$$

where

$(hkl)_s$ = a low-index plane of the substrate,
$[uvw]_s$ = a low-index direction in $(hkl)_s$,
$(hkl)_n$ = a low-index plane in the nucleating solid,
$[uvw]_n$ = a low-index direction in $(hkl)_n$,
$d[uvw]_n$ = the interatomic space along $[uvw]_n$,
$d[uvw]_s$ = the interatomic space along $[uvw]_s$.

From Eq. (1), a simpler equation can be derived for the plane and direction with the lowest mismatch between the substrate (potential heterogeneous nucleation site) and the nucleating solid which is labelled as lattice parameter mismatch (f). The lattice parameter mismatch (f) reported in Table 1 was calculated using Eq. (2) [32,33]:

$$f = \frac{\text{lattice constant of solid} - \text{lattice constant of substrate}}{\text{lattice constant of substrate}} \quad (2)$$

From the data shown in Table 1, it can be seen that Nb has higher melting point and slightly lower lattice parameter mismatch with Al in comparison to Ti which would favour the solidification of molten Al. Another important point is that the intermetallic Al_3Nb is characterised by a tetragonal structure with 8 atoms per unit cell exactly as the Al_3Ti phase and they have equal lattice mismatch with Al.

3.1.2. Effect of Nb addition on pure Al

Initially, a first set of experiments was carried out to study and confirm the promising potential of Nb as grain refiner and for that commercial pure Al was considered. In particular, pure Al was melted at 720 °C and different percentages of Nb (0.1–15 wt.%) in the form of powder (average particle size of 100 μm) were added to the melt, left to dissolve for at least 1 h mixing the melt several times and slow cooled (cooling rate ~0.3 °C/s). The results of the experiments carried out to study the effect of the addition of different level of Nb to Al are summarised in the micrographs shown in Fig. 2.

At it can be seen from the results shown in Fig. 2, even though of its promising characteristics as potential nucleation site, the preliminary experiments with the addition of Nb (0.1–15 wt.%) to pure Al melt were not satisfactory because relatively large primary Al α-grains generally in the order of 1–5 mm were obtained. This unsatisfactory result could be mainly due to two factors: the poor dissolution of Nb in Al and the higher density of Nb with respect to Al.

3.1.3. Effect of solidification temperature combined with Nb inoculation

The dissolution process of solid in liquid metal is commonly described by the Nernst–Shchukarev equation and, consequently, the bulk concentration in the melt changes according to an exponential law (Eq. (3) [35]):

$$C = C_S\left[1 - \exp\left(-\frac{k \cdot s \cdot t}{v}\right)\right] \quad (3)$$

where C is the concentration of the dissolved metal in the bulk of the melt measured at the time (t), C_S is the saturation concentration, k is the dissolution rate constant, s is the specimen surface area and v is the volume of the melt. The values of the solubility (K) of Nb in Al calculated on the base of Eq. (3) are available in the literature [36] and are reported in Table 2 with the values of the dissolution rate constant (K_1) and the coefficient of diffusion (D).

As it can be seen from the data shown in Table 2, the maximum solubility of Nb in Al increases with the processing temperature

Table 1
Comparison of lattice structures and relative lattice parameter mismatch f used for the development of the novel Nb–B grain refiner [34].

Element	Phase	Melting point (°C)	Density (g/cm^3)	Lattice structure	Lattice parameter	f (%)
Aluminium	Al	660	2.7	Face-centred cubic	a = 4.050 Å	–
Titanium	Ti	1668	4.51	Hexagonal	a = 2.950 Å, c = 4.683 Å	37.3
	Al_3Ti	1350	3.36	Tetragonal	a = 3.848 Å, c = 8.596 Å	4.2
	TiB_2	3230	4.52	Hexagonal	a = 3.023 Å, c = 3.220 Å	34
	TiC	3160	4.93	Face-centred cubic	a = 4.330 Å	−6.5
Niobium	Nb	2468	8.57	Body-centred cubic	a = 3.300 Å	22.7
	Al_3Nb	1680	4.54	Tetragonal	a = 3.848 Å, c = 8.615 Å	4.2
	NbB_2	3036	6.98	Hexagonal	a = 3.102 Å, c = 3.285 Å	30.6
	NbC	3490	7.82	Face-centred cubic	a = 4.430 Å	−8.6

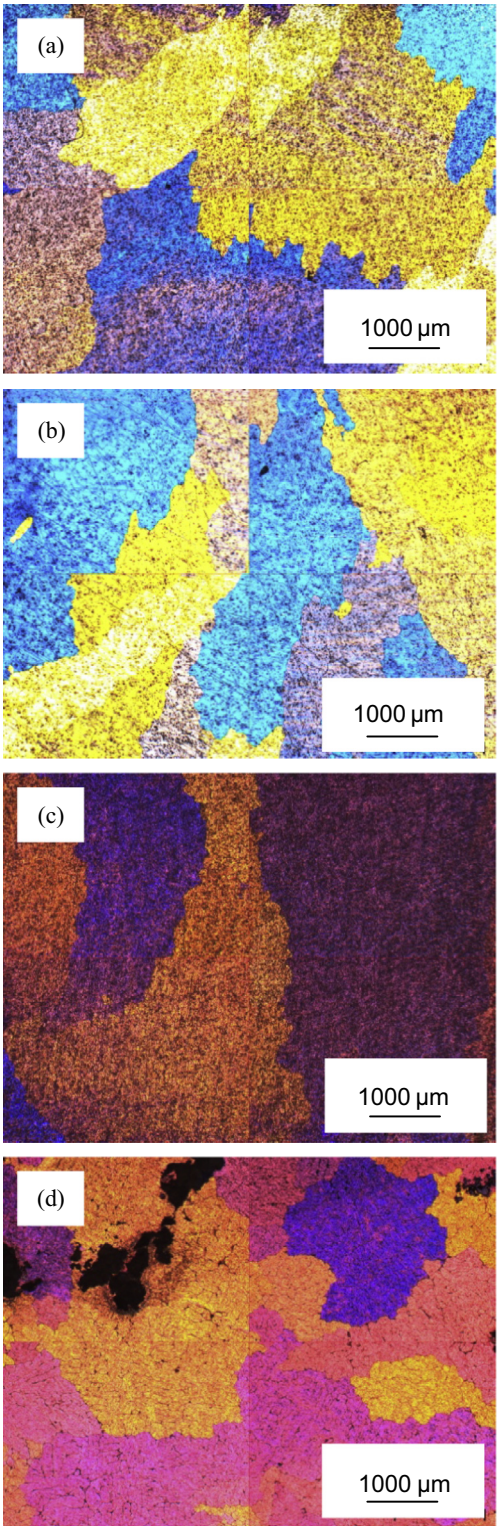

Fig. 2. Micrographs of pure aluminium slow cooled (cooling rate ~0.3 °C/s) from 720 °C and with different niobium addition: (a) reference, (b) 0.1 wt.%, (c) 2 wt.% and (d) 15 wt.%.

and, thus, a new set of experiments were programmed. Specifically, Nb content was set to 1 wt.%, the solidification temperature of pure Al melted at 750 °C was ranged between 660° and 720 °C and the samples were left to solidify inside the crucible (cooling rate ~0.3 °C/s). A representative example of the results from these set of experiments are summarised in Fig. 3 by means of the

Table 2
Solubility of niobium in aluminium as a function of the processing temperature [36].

	T (°C)			
	700	750	800	850
Solubility, K (wt.%)	0.02	0.034	0.057	0.1
Dissolution rate constant, K_1 (m/s)	4.6	5.1	6.2	6.8
Coefficient of diffusion, $D \cdot 10^9$ (m^2/s)	1.61	1.86	2.49	2.89

macroetched cross-sections of the casts where the sedimented Nb particles were found.

From the macrographs shown in Fig. 3 it can be noticed that there is not a significant refinement with the addition of Nb if not in the bottom part of the solidified metal. In order to prove that the grain refinement of the bottom part of the metal left to solidify inside the crucible is actually due to the presence of Nb particles, the cross-section of the casts were cut, polished and microscopically analysed and the results are shown in Fig. 3b).

3.1.4. Comparison of the addition of Al–Ti–B and Nb to commercially pure Al

In order to favour the dissolution of Nb into the molten Al, the processing temperature was increased to 800 °C, the particle size of the Nb powder was reduced (<45 μm) and the holding time was prolonged to 2 h. These dissolution conditions were employed for the comparison of the grain refinement efficiency of the Nb addition with that of the commercial Al–5Ti–B master alloy using TP-1 tests (pouring temperature: 680 °C). Fig. 4 shows the comparison of the size of the primary α-Al grains without and with the addition of 0.1. wt.% of Nb or commercial Al–5Ti–1B master alloy.

The quantification of the α-Al grain size (Fig. 4) revealed that the solidification of pure Al under the conditions specified in the TP-1 test leads to quite coarse grain size (i.e. 1700 ± 40 μm). The addition of the grain refiners, both the commercial Al–5Ti–1B master alloy and Nb, drastically reduces the grain size of commercially pure Al of about one order of magnitude. Moreover, the commercial grain refiner performs better (i.e. 300 ± 25 μm) in comparison to the addition of Nb (i.e. 1210 ± 15 μm).

3.2. Study of the addition of interstitials (B and C) to the Al–Nb system

3.2.1. Analogies/differences between the Al–Ti–B/Al–Nb–B and Al–Ti–C/Al–Nb–C ternary systems

Keeping in mind that the development of grain refiners was based on the proposed nucleation theories for the Al–Ti–B system [7–9] where the combined presence of Ti and B is responsible for the grain refinement, the combined addition of Nb with interstitials such as B and C was considered. The addition of these interstitial elements should lead to the formation of niobium boride (NbB_2) and niobium carbide (NbC), respectively. As it can be seen from the data reported in Table 1, TiB_2 and NbB_2 are characterised by the same crystal structure (hexagonal) and have similar lattice parameter mismatch with Al and NbC has a similar structure and lattice parameter mismatch of TiC. Specifically, the lattice mismatch of TiB_2 is slightly higher than that of NbB_2 whilst that of TiC is somewhat lower than that of NbC. The formation and the presence of these hard refractory ceramic particles inside the Al melt should favour the grain refinement of Al by heterogeneous nucleation.

3.2.2. Effect of the addition of Nb–B and Nb–C to commercially pure Al

Pure Al was melted at 750 °C and left to homogenise during 1 h. Afterwards, the Nb powder (<45 μm) plus either B powder or C powder were added to the melt and left to dissolve for at least 1 h with several intermediate mixing. The melt were left to cool

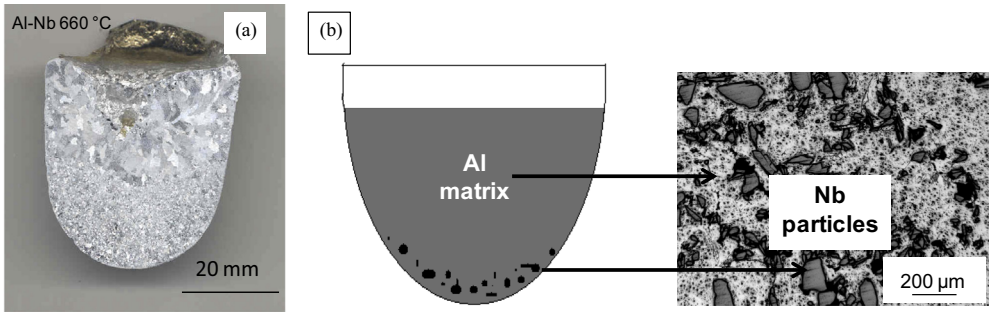

Fig. 3. Macrographs of pure aluminium with the addition of 1 wt.% of niobium (a) and (b) scheme and micrograph of the polished cross-section of the bottom part of the cast Al with Nb particles.

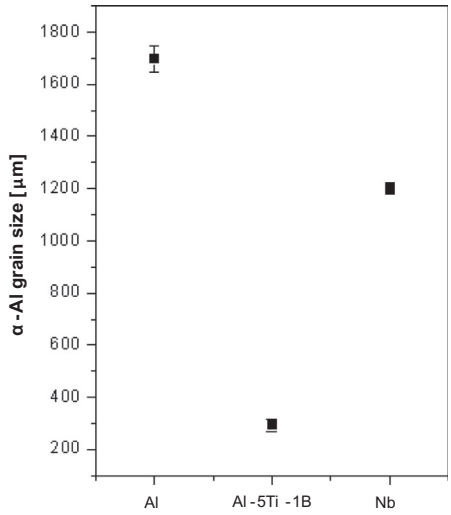

Fig. 4. Comparison of the grain size of pure aluminium with and without addition of 0.1 wt.% of Al–5Ti–1B and 0.1 wt.% of Nb (TP-1 test at 680 °C).

inside the crucibles (cooling rate ~0.3 °C/s). Fig. 5 shows the comparison of the microstructural features between pure Al without and with the addition of Nb and B or C.

As it can be seen in Fig. 5a), commercially pure Al slow cooled inside the crucible is characterised by a very big primary Al α-grains in the order of millimetres. On the one side, the inoculation by the combined addition of Nb and C (Fig. 5b) has very little effect on the grain refinement of commercially pure Al because the size of the primary Al α-grains is of the same order of that of Al without addition of any grain refiner. On the other side, the addition of Nb–B to Al (Fig. 5c) induces a significant reduction of the primary α-Al structure resulting in an average grain size of approximately 350 µm. From this set of experiments it can be evinced that the grain refinement effect of Nb is significantly enhanced by the addition of B but not C.

3.2.3. Optimisation of the B addition

It was found that the addition of the B powder to the Al melt is a limiting factor due to the non-wetting behaviour of B in liquid Al and to the difference in terms of density. Specifically, B floats in the surface of the molten Al because its density (2.08 g/cm^3) is lower than that of Al (2.7 g/cm^3). A common industrial practise is the use potassium fluorides to introduce the alloying elements needed to fabricate the grain refinement. An example is the employment of potassium tetrafluoroborate (KBF_4) and potassium hexafluorotitanate (K_2TiF_6) fluxes to obtain the commercial Al–5Ti–1B master alloy generally used as grain refiner for wrought

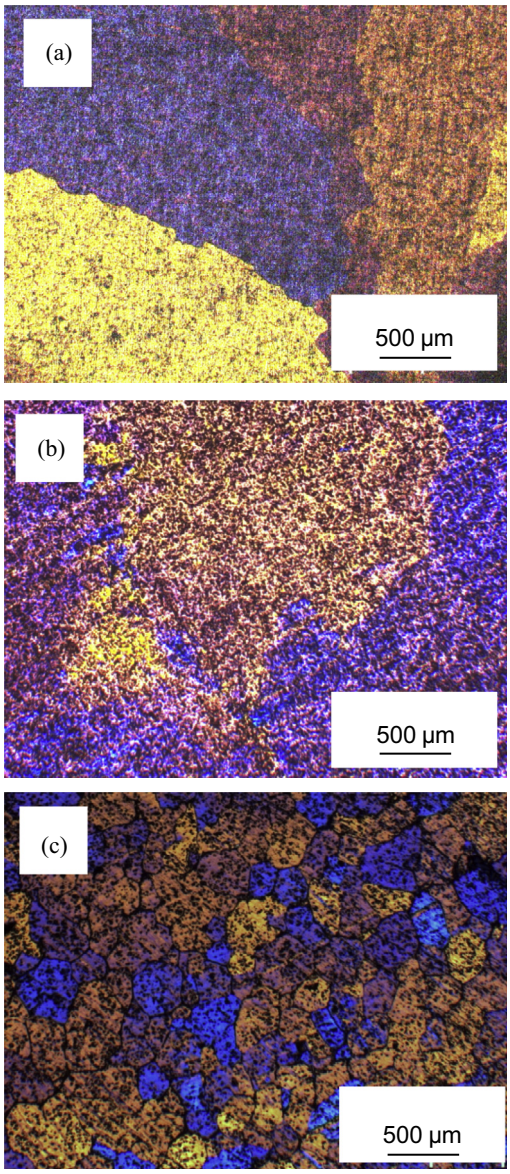

Fig. 5. Micrographs of pure aluminium cooled without and with the addition of niobium and boron or carbon (cooling rate ~0.3 °C/s): (a) Al, (b) Al + (Nb–C) and (c) Al + (Nb–B).

Al alloys. The individual reactions that govern this industrial process are reported in Eqs. (4)–(6) whilst the net reaction is shown in Eq. (7):

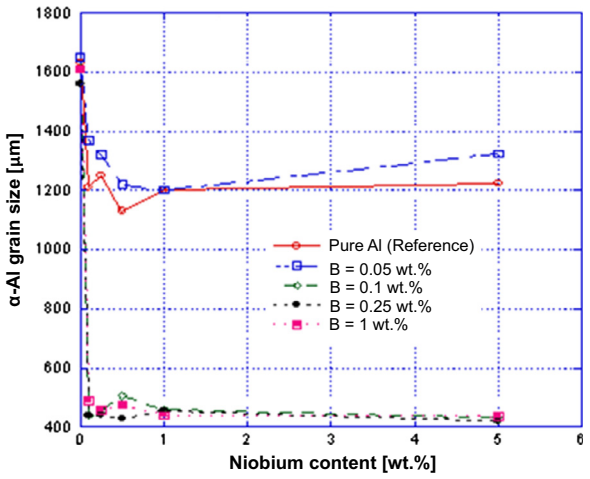

Fig. 6. Variation of the primary Al α-grain size with the amount of Nb and B, in the form of KBF_4, added to the melt (TP-1 test at 680 °C).

$$3K_2TiF_6 + 13Al \rightarrow 3Al_3Ti + 3KAlF_4 + K_3AlF_6 \quad (4)$$

$$2KBF_4 + 3Al \rightarrow AlB_2 + 2KAlF_4 \quad (5)$$

$$Al_3Ti + AlB_2 \rightarrow TiB_2 + 4Al \quad (6)$$

$$6K_2TiF_6 + 6KBF_4 + 23Al \rightarrow 3TiB_2 + 3Al_3Ti + 18KF + 14AlF_3 \quad (7)$$

Similarly, in the case of addition of pure Nb powder and potassium tetrafluoroborate to molten Al, the individual reactions can be described by means of Eqs. (5), (8) and (9) and the global reaction by Eq. (10):

$$Nb + 3Al \rightarrow Al_3Nb \quad (8)$$

$$Al_3Nb + AlB_2 \rightarrow NbB_2 + 4Al \quad (9)$$

$$2Nb + 2KBF_4 + 5Al \rightarrow NbB_2 + Al_3Nb + 2KF + 2AlF_3 \quad (10)$$

The employment of potassium tetrafluoroborate flux is not only advantageous from the point of view of introducing B into the molten Al preventing the floating of the powder but it also contributes to the dissolution of the Nb powder particles. This is because the reaction taking place between Al and the potassium tetrafluoroborate salt is exothermic and, therefore, locally the temperature inside the melt is much higher. The local increment of the temperature increases the solubility as well as diffusion rate of Nb in Al (see Table 2) and, thus, it will boost up the dissolution of the Nb powder particles added to the melt.

Once identified the best source for adding B and confirmed that the procedure employed guarantee the complete dissolution of Nb, the attention was focused on the optimisation of the amount of B to be added for an effective grain refinement. For this set of experiments, pure Al was melt at 800 °C, Nb powder addition was varied between 0.01 wt.% and 5 wt.% whilst the total amount of B, in the form of KBF_4, added was ranged between 0.05 wt% and 1 wt.%. After one hour of homogenisation, TP-1 tests were done at a pouring temperature of 680 °C. The results of the optimisation of the Nb/B addition are presented in Fig. 6.

Form Fig. 6, it can be noticed that the addition of Nb or B alone has also a very little effect on the final grain size of Al. When considering the Nb–B inoculation of Al (Fig. 6), it can be seen that the Nb–B mixture is very effective for grain refinement with the exception of the products where the lowest amount of B considered (i.e. 0.05 wt.%) is employed whose grain size is comparable to that of the reference material and/or the addition of exclusively Nb.

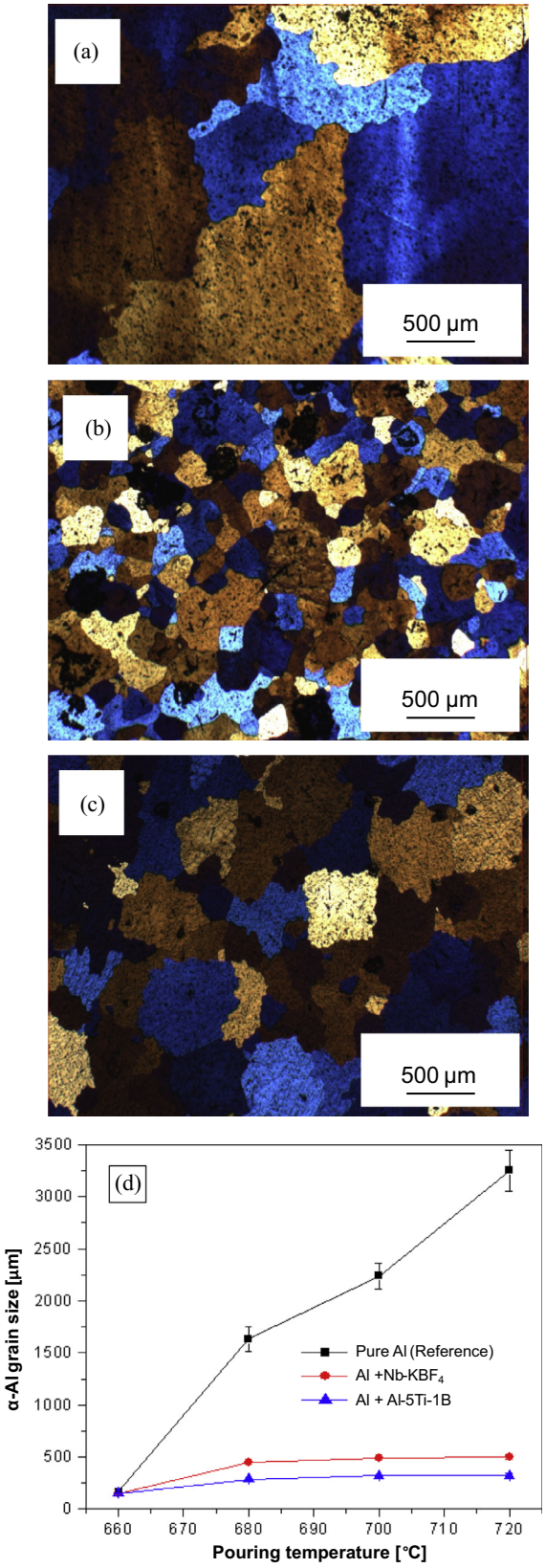

Fig. 7. Micrographs of commercially pure aluminium solidified 680 °C: (a) reference, (b) 0.1 wt.% of Al–5Ti–1B and (c) addition of 0.1 wt.% Nb–B powders (0.1Nb–0.1B) and (d) variation of the α-Al grain size with the pouring temperature.

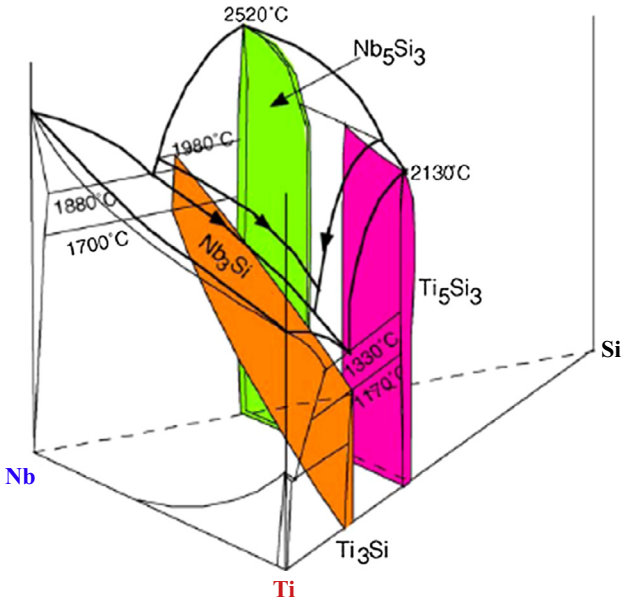

Fig. 8. The Ti–Nb–Si ternary system (adapted from [37]) showing that Ti–Si compounds form and are stable at lower temperatures in comparison to Nb–Si compounds.

3.2.4. Comparison of the addition of Al–Ti–B and Nb–B to commercially pure Al

On the base of the results of the variation of the grain size as a function of the combined effect of Nb and B (Fig. 6), the amount of these two elements was set to 0.1 wt.% (0.1Nb–0.1B) because this is the lowest percentage which guarantees the grain refinement without significantly change the chemical composition of the material. In these set of experiments the addition of the commercial Al–5Ti–1B master alloy to pure Al was compared with that of the 0.1Nb–0.1B powders addition (TP-1 test). Representative micrographs of the results of the experiments done are shown in Fig. 7a–c) whilst the variation of the primary Al α-grain size is graphed in Fig. 7d).

As it can be seen from the results presented in Fig. 7, there is not any significant difference in terms of grain size between the commercially pure Al without and with the addition of any grain refiner when considering a solidification temperature of 660 °C because the average grain size is approximately 200 μm. Nonetheless, it can be noticed that the mean primary Al α-grain size significantly increases with the increment of the pouring temperature reaching almost 3300 μm without the addition of any grain refiners whereas the increment of the grain size is far less limited after addition. Moreover, it can be seen that the difference in grain size between the reference material and the grain refined materials also increases with the solidification temperature reaching one order of magnitude (i.e. 300 μm vs. 3000 μm) at 720 °C. When considering the effect of the each grain refiners, it can be seen that the commercial Al–5Ti–1B master alloy performs slightly better than the 0.1Nb–0.1B powders because there is a constant difference of approximately 200 μm in between them independently of the pouring temperature studied.

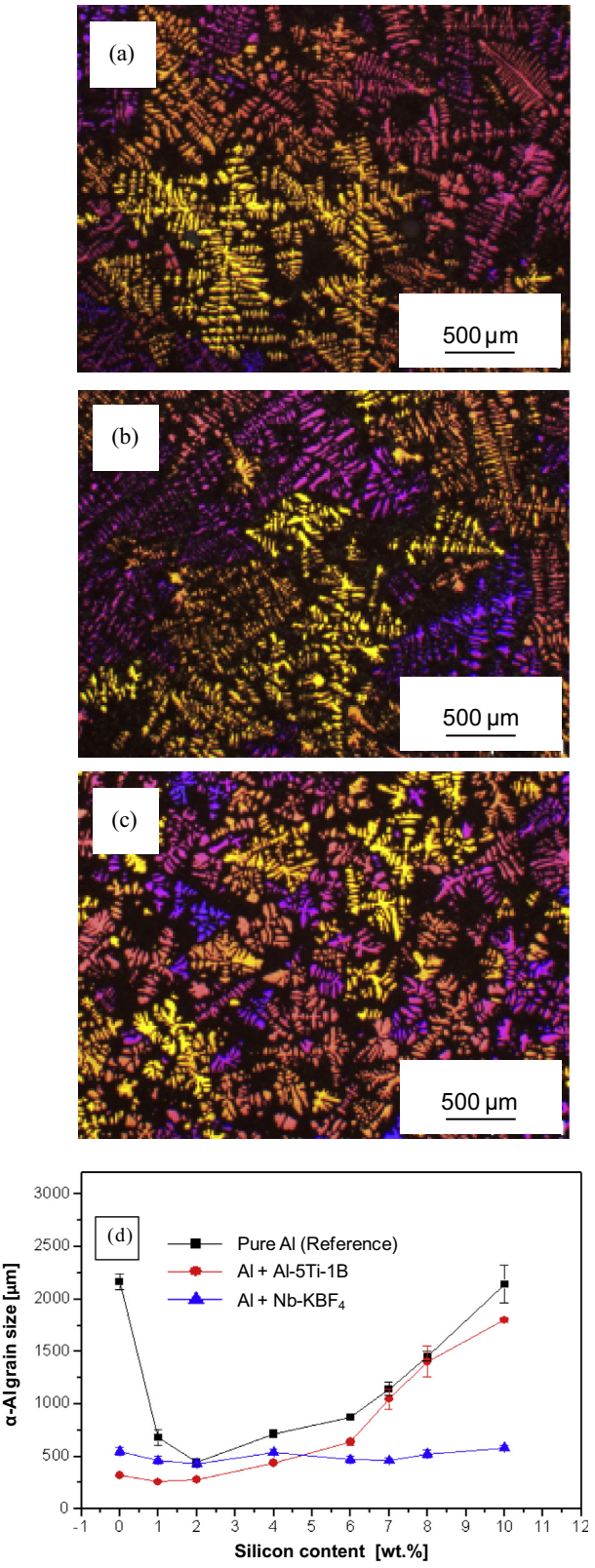

Fig. 9. Micrographs of binary Al–7Si alloys cast at 700 °C: (a) reference, (b) 0.1 wt.% Al–5Ti–1B, (c) 0.1 wt.% Nb–B and (d) comparison of the variation of the primary Al α-grain size with the silicon content.

3.3. Study of the addition of the 0.1Nb–0.1B grain refiner to Al–xSi binary alloys

3.3.1. Analogies/differences between the Ti–Si and Nb–Si binary systems

As reported in the introduction, the grain refinement of Al–Si alloys cannot be performed efficiently by Al–Ti–B master alloys because when the Si percentage is greater than 4 wt.%, Ti and Si react leading to the formation of silicides (poisoning). A better understanding of the compounds that form between Ti, Si and

Nb can be achieved by studying the Ti–Nb–Si ternary phase diagram (Fig. 8).

From the Ti–Si binary phase diagram (Fig. 8) five titanium silicides (Ti_3Si, Ti_5Si_3, Ti_5Si_4, TiSi and $TiSi_2$) can be formed. In the case of the binary Nb–Si phase diagram (Fig. 8) it can be noticed that Nb has a similar behaviour to Ti and three intermetallic compounds, precisely Nb_5Si_3, Nb_3Si and $NbSi_2$, can form. Nevertheless, there is a very important difference among the two binary phase diagrams and it is that Ti_3Si is stable at much lower temperature (<1170 °C) as compared to Nb_3Si which is stable between ~1700 °C and 1980 °C (Fig. 8) [37]. It is worth mentioning that, in general, niobium silicides are high temperature intermetallics whose melting temperature is higher with respect to that of titanium silicides. As it was found experimentally, Si has very little solubility in both $AlNb_3$ and $AlNb_2$ intermetallics, and only ~2 at.% in Al_3Nb [38]. This suggests that an Al melt at 800 °C there will be extremely less probability to form niobium silicides than titanium silicides and, therefore, the Nb-based phases would act as heterogeneous nucleation sites for Al without poisoning.

3.3.2. Comparison of the addition of Al–Ti–B and Nb–B to hypoeutectic binary Al–xSi alloys

In order to clearly identify the effect of the addition of the Nb–B refiner, binary Al–*x*Si alloys were studied. It is worth mentioning that, commonly, commercial Al–Si cast alloys used in industry have a Si content greater than 4 wt.%. Nonetheless, in this study Al–1Si and Al–2Si alloys were also produced and studied to better understand and characterise the Nb–B inoculation behaviour. The results of the characterisation of the TP-1 tests done from a pouring temperature of 700 °C are summarised in Fig. 9. In particular, a comparison of the microstructural features by means of micrographs of selected binary Al–7Si and of the variation of the primary Al α-grain size with the Si content is presented.

From Fig. 9 it can be seen that the refinement of the binary Al–7Si alloy (Fig. 9a) through the addition of commercial Al–5Ti–1B master alloys (Fig. 9b) is not effective because both materials are characterised by a very coarse dendritic microstructure. Conversely, the grain refinement with the 0.1Nb–0.1B refiner (Fig. 9c) leads to a much finer microstructural features. From a Si content of about 4 wt.% the primary Al α-grain size continuously increases and the binary Al–10Si alloy has similar grain size (2150 μm) to that of pure Al. In the case of the commercial Al–5Ti–1B master alloy addition, the primary Al α-grain size increase continuously starting from a Si content following the same trend of the binary Al–*x*Si alloys and reaching a maximum value of 1850 μm in the binary Al–10Si alloy. Considering the addition of the 0.1Nb–0.1B refiner in the form of powders, it can be noticed that this is highly efficient in refining commercially pure Al, because the grain size is reduced of one order of magnitude. Nonetheless, the most important point is that Nb–B inoculation leads to the grain refinement of binary Al–*x*Si alloys throughout the whole spectrum of Si content analysed (i.e. 1–10 wt.%).

3.3.3. Effect of the Nb–B inoculation in binary Al–xSi alloys on the base of thermal analysis

Thermal analysis has been used to assess the performance of grain refiners and it is an efficient tool to determine the refining efficiency of a grain refiner [8]. Fig. 10 shows the cooling curves of the binary Al–5Si alloy without and with Nb–B inoculation studied to measure the undercooling and the nucleation temperature of the primary Al α-grains as well as to determine whether heterogeneous nucleation is the main mechanism of solidification.

Concerning the data of the thermal analysis (Fig. 10 and Table 3), the nucleation temperature (T_N) is identified as the point where the cooling curve starts to deviate from linearity. This is the temperature when the first Al crystal nucleates and starts to grow in the

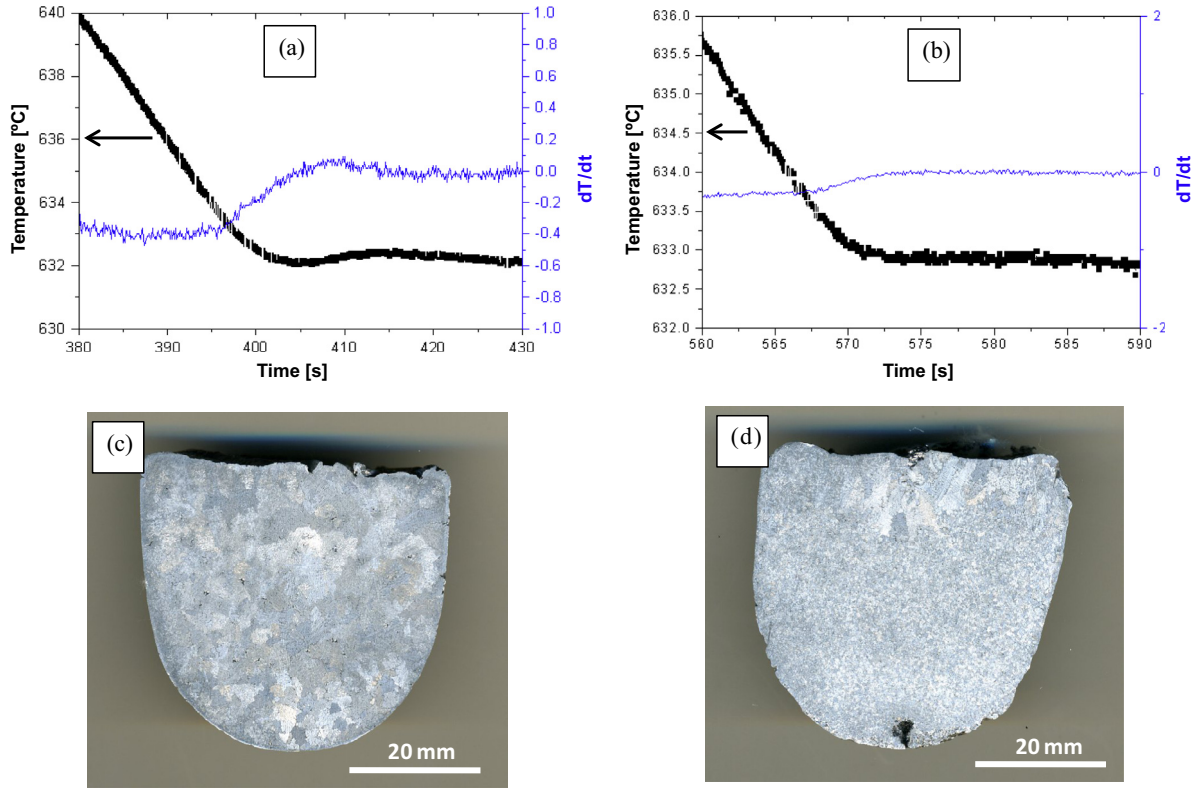

Fig. 10. Comparison of the cooling curves (cooling rate ~0.3 °C/s) of the binary Al–5Si alloy: (a) without and (b) with Nb–B inoculation and macroetched surface of the binary Al–5Si alloy: (c) without and (d) with Nb–B inoculation.

Table 3
Primary α-Al or eutectic nucleation temperature (T_N), minimum temperature (T_{min}), growth temperature (T_G) and undercooling for primary α-Al nucleation or recalescence for eutectic nucleation (ΔT) as measured from the cooling curves shown in Fig. 10.

		T_N (°C)	T_{min} (°C)	T_G (°C)	ΔT (°C)
α-Al nucleation	Al–5Si	633.2	631.9	632.3	0.4
	Al–5Si + Nb–B	633.7	632.7	632.8	0.1
Eutectic nucleation	Al–10Si	578.8	575.5	575.8	0.3
	Al–10Si + Nb–B	574.3	572.7	573.9	1.2

case of the primary Al α-grains and the temperature when the first eutectic Si crystal nucleates and starts to grow in the case of the eutectic phase. The other two measured temperatures, T_{min} and T_G, are defined as the minimum and maximum reaction temperatures of either the primary α-Al or eutectic nucleation, respectively. Consequently, $\Delta T = (T_G - T_{min})$ is the undercooling in the case of the primary α-Al nucleation and describes the recalescence of the eutectic arrest in the case of the eutectic nucleation [39]. From the analysis of the data concerning the primary α-Al nucleation (Fig. 10a and b and Table 3), it can be seen that Nb–B inoculation leads to a somewhat higher nucleation temperature but the most important point is that the undercooling is lower in comparison to the untreated alloy (Al–5Si). A perfect heterogeneous nucleating site would reduce the activation energy for nucleation to zero. Thus, the extent of undercooling is indirectly proportional to the efficiency of a grain refiner in providing potent nucleating sites [8]. From the literature available for the grain refinement of Al–Si alloys, it is suggested that a good grain refinement is achieved when the undercooling is below 0.3 °C [40]. In the case of Nb–B inoculation, the undercooling is lowered in comparison to the untreated materials indicating that it is actually a potent nucleation agent which induces heterogeneous nucleation. From the analysis of the macroetched surface of the binary Al–5Si alloy it was found that the Nb–B inoculation is highly effective even at very slow cooling rate. Specifically, the mean primary α-Al grain size of the untreated Al–5Si alloy (Fig. 10c) is approximately 2500 ± 130 μm whereas Nb–B inoculation leads to a grain size of about 380 μm.

The cooling curve of the binary Al–10Si alloy is presented in Fig. 11 where it can be seen that Nb–B inoculation lowers the eutectic nucleation temperature and leads also to a greater recalescence. Specifically, the untreated alloy shows low recalescence prior to eutectic growth (~0.3 °C) whereas after Nb–B inoculation the material has a ΔT of 1.2 °C.

It is well known that the larger the magnitude of the recalescence, the higher the level of modification [41]. The term "modification" identifies the addition of chemicals to induce the change of the morphology of the Al–Si eutectic phase normally composed of large plates and some lamellar structure (faceted phase) to a much finer and fibrous eutectic flake-like phase. The most common elements used in industry for the modification of the coarse plate-like eutectic phase of Al–Si cast alloys are strontium and sodium [39]. The results of the eutectic nucleation after Nb–B inoculation indicates that this composition is not only highly effective for the refining of the primary α-Al grain structure of Al–Si cast alloys but, simultaneously, has some effect (i.e. refine but not modify) on the Al–Si eutectic phase of the binary Al–*x*Si alloys. The analysis of the micrographs of the untreated Al–10Si alloy (Fig. 11c) shows that the microstructure is composed of dendritic coarse primary α-Al grains (around 2000 μm), quite large and unevenly distributed eutectic needles (50–80 μm) and quite large amount of primary Si particles of approximately 20 μm. As expected on the base of the data plotted in Fig. 9d), Nb–B inoculation in the binary Al–10Si alloy significantly reduces the primary α-Al grain size (Fig. 11d). Nevertheless, the microstructural analysis confirms also that the addition of Nb–B to Al–*x*Si alloys is also able to refine the eutectic phase which switches to an even distribution of fine intermetallic particles of about 10–30 μm.

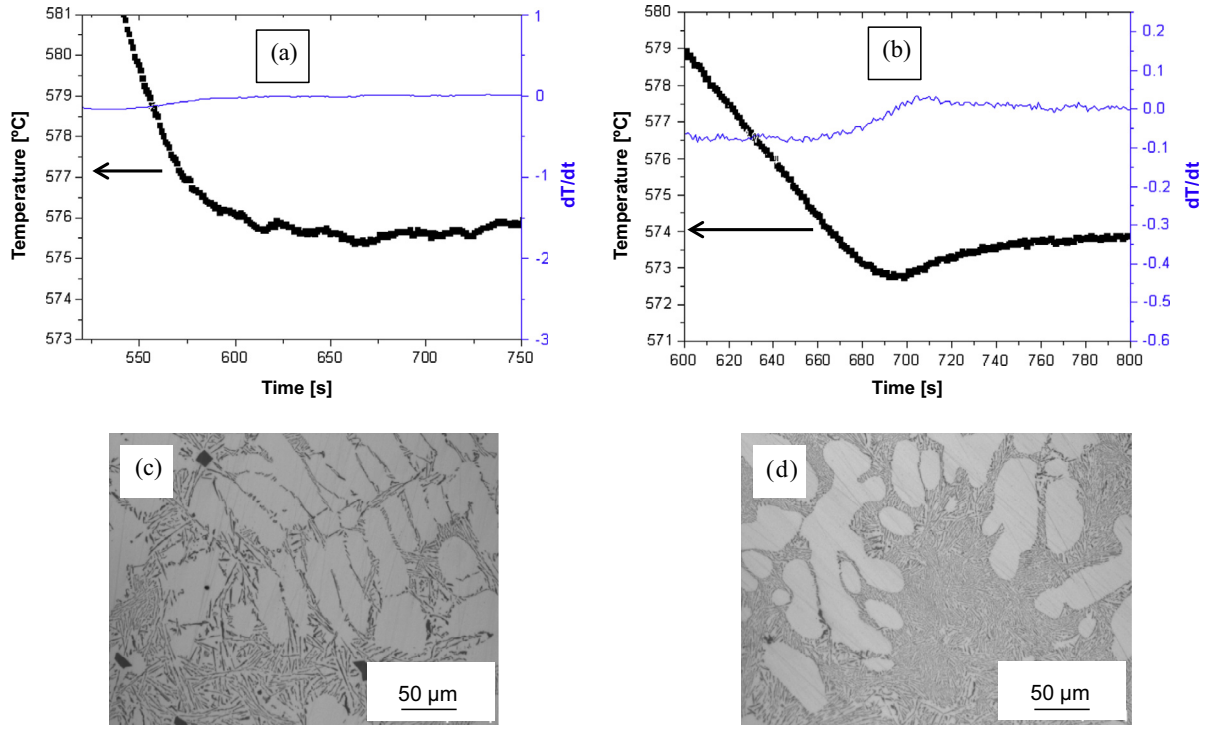

Fig. 11. Detail of the binary Al–10Si alloy cooling curve where the eutectic nucleation takes place: (a) without and (b) with Nb–B inoculation and micrograph of Al–10Si: (c) without and (d) with Nb–B inoculation.

4. Conclusions

From the study of the addition of Nb both alone and in combination with B to Al and Al–Si alloys it can be concluded that:

- The Al–Nb binary diagram is characterised by a peritectic reaction which permits the formation of Nb aluminide particles which are able to refine the microstructure of commercially pure Al. Nevertheless, Nb is not as efficient as Ti or the commercial Al–Ti–B master alloy due to its higher lower growth restriction factor.
- The combined addition of B and Nb to commercially pure Al leads to finer microstructure in comparison to the untreated material due to the reduction of the constitutional undercooling. The final grain size is comparable, slightly coarser, to that obtained by adding commercial Al–Ti–B master alloy.
- The developed Nb–B grain refiner can efficiently refine binary Al–*x*Si alloys due to the formation of niobium borides which are more stable than titanium borides, therefore, significantly limiting the so called poisoning effect. The best performance of the novel Nb–B grain refiner is for Al–Si alloy with Si content greater than 6 wt.%.
- The addition of the novel Nb–B grain refiner does not only leads to finer primary Al α-grains but also to finer Al–Si eutectic phase due to the more homogeneous distribution of the alloying elements in the solidification front and eutectic pools.

Acknowledgement

The authors are thankful for the financial support from the Engineering and Physical Sciences Research Council (EPSCR) through the EP/J013749/1 Project.

References

[1] Rooy EL. Aluminum and aluminum alloys, castings. vol. 15. Ohio: ASM International; 1988.
[2] Sigworth GK. The grain refining of aluminum and phase relationships in the Al–Ti–B system. Metall Trans A 1984;15:277–82.
[3] Guzowski MM, Sigworth GK, Sentner DA. The role of boron in the grain refinement of aluminum with titanium. Metall Trans A 1987;18:603–19.
[4] Sritharan T, Li H. Influence of titanium to boron ratio on the ability to grain refine aluminium–silicon alloys. J Mater Process Technol 1997;63:585–9.
[5] Greer AL, Cooper PS, Meredith MW, Schneider W, Schumacher P, Spittle JA, et al. Grain refinement of aluminium alloys by inoculation. Adv Eng Mater 2003;5:81–91.
[6] Easton M, St John D. An analysis of the relationship between grain size, solute content, and the potency and number density of nucleant particles. Metall Trans A 2005;36:1911–20.
[7] McCartney DG. Grain refining of aluminium and its alloys using inoculants. Int Mater Rev 1989;34:247–60.
[8] Murty BS, Kori SA, Chakraborty M. Grain refinement of aluminium and its alloys by heterogeneous nucleation and alloying. Int Mater Rev 2002;47:3–29.
[9] Easton M, St. John DH. Grain refinement of aluminum alloys: Part I. The nucleant and solute paradigms – a review of the literature. Metall Mater Trans A 1999;30:1613–23.
[10] St John DH, Hogan LM. Al_3Ti and the grain refinement of aluminum. J Aust Inst Met 1977;22:160–6.
[11] Schumacher P, Mc Kay BJ. TEM investigation of heterogeneous nucleation mechanisms in Al–Si alloys. J Non-Cryst Solids 2003;317:123–8.
[12] Sigworth GK, Guzowski MM. Grain refining of hypoeutectic Al–Si alloys. AFS Trans 1985;93:907–12.
[13] Spittle JA, Sadli S. Effect of alloy variables on grain refinement of binary aluminium alloys with Al–Ti–B. Mater Sci Technol 1995;11:533–7.
[14] Kori SA, Auradi V, Murty BS, Chakraborty M. Poisoning and fading mechanism of grain refinement in Al–7Si alloy. Mater Forum 2005;29:387–93.
[15] Sicha WE, Boehm RC. Grain refinement in Al–4.5% Cu alloys. AFS Trans 1948;56:398–409.
[16] Crossley FA, Mondolfo LF. Mechanism of grain refinement in aluminum alloys. J Met (Trans AIME) 1951;191:1143–8.
[17] Cibula A, Ruddle RW. The effect of grain size on the tensile properties of high strength cast aluminum alloys. J Inst Met 1949–1950;76:361–76.
[18] Clyne TW, Nazar AMM, Prates M, Davis GJ. Grain refinement of aluminium using niobium additions. Mater Sci Technol 1978;5:302–8.
[19] Shabani MJ, Emamy M, Nemati N. Effect of grain refinement on the microstructure and tensile properties of thin 319 Al castings. Mater Des 2011;32:1542–7.
[20] Gezer BT, Toptan F, Daglilar S, Kerti I. Production of Al–Ti–C grain refiners with the addition of elemental C. Mater Des 2010;31:S30–5.
[21] Li P, Liu S, Zhang L, Liu X. Grain refinement of A356 alloy by Al–Ti–B–C master alloy and its effect on mechanical properties. Mater Des 2013;47:522–8.
[22] Zhang Y, Ma N, Wang H, Li X. Study on damping behavior of A356 alloy after grain refinement. Mater Des 2008;29:706–8.
[23] Samuel E, Golbahar B, Samuel AM, Doty HW, Valtierra S, Samuel FH. Effect of grain refiner on the tensile and impact properties of Al–Si–Mg cast alloys. Mater Des 2014;56:468–79.
[24] Birol Y. Performance of $AlTi_5B_1$, $AlTi_3B_3$ and AlB_3 master alloys in refining grain structure of aluminium foundry alloys. Mater Sci Technol 2012;28:481–6.
[25] Hari Babu N, Shi Y, Iida K, Cardwell DA. A practical route for the fabrication of large single-crystal (RE)-Ba–Cu–O superconductors. Nat Mater 2005;4:476–80.
[26] Nowak M. Development of niobium–boron grain refiner for aluminium–silicon alloys. Ph.D. thesis, Brunel University, London, UK; 2011. <http://bura.brunel.ac.uk/handle/2438/8321> [accessed July 2014].
[27] Hari Babu N, Nowak M. Method of refining metal alloys; 2012. Patent N°: WO2012110788. <http://patentscope.wipo.int/search/en/WO2012110788> [accessed July 2014].
[28] The Aluminum Association. TP-1 – standard test procedure for aluminum alloy grain refiners. Washington DC, USA; 2002.
[29] Mondolfo LF. Aluminium alloys: structure and properties. Boston: Butterworths; 1976.
[30] Greer AL, Bunn AM, Tronche A, Evans PV, Bristow DJ. Modelling of inoculation of metallic melts: application to grain refinement of aluminium by Al–Ti–B. Acta Mater 2000;48:2823–35.
[31] Bramfitt BL. The effect of carbide and nitride additions on the heterogeneous nucleation behavior of liquid iron. Metall Mater Trans B 1970;1:1987–95.
[32] Burke JE, Turnbull D. Recrystallization and grain growth. Prog Met Phys 1952;3:220–92.
[33] Frank FC, van der Merwe JH. One-dimensional dislocations. I. Static theory. Proc R Soc A London 1949:205–25.
[34] Totten GE, Scott Mac Kenzie D. Handbook of aluminium. Alloy production and materials manufacturing, vol. 2. New York – Basel: Marcel Dekker Inc.; 2003.
[35] Yeremenko VN, Natanzon YV, Dybkov VI. The effect of dissolution on the growth of the Fe_2Al_5 interlayer in the solid iron–liquid aluminium system. Prog Met Phys 1981;16:1748–56.
[36] Yerembnko VN, Natanzon YV, Dybkov VI. Interaction of the refractory metals with liquid aluminium. J Less Common Met 1976;50:29–48.
[37] Zhao JC, Jackson MR, Peluso LA. Mapping of the Nb–Ti–Si phase diagram using diffusion multiples. Mater Sci Eng A 2004;372:21–7.
[38] Pan VM, Latysheva VI, Kulik OG, Popov AG, Litvinenko EN. Nb–$NbAl_3$–Nb_5Si_3 phase diagram. Russian Metall (Metally) 1984;4:233–5.
[39] Knuutinen A, Nogita K, McDonald SD, Dahle AK. Modification of Al–Si alloys with Ba, Ca, Y and Yb. J Light Met 2001;1:229–40.
[40] Apelian D, Sigworth GK, Whaler KR. Assessment of grain refinement and modification of Al–Si foundry alloys by thermal analysis. AFS Trans 1984;92:297–307.
[41] Djurdjevic M, Jiang H, Sokolowski J. On-line prediction of aluminum–silicon eutectic modification level using thermal analysis. Mater Charact 2001;46:31–8.